T–S Model-Based SMC Reliable Design for a Class of Nonlinear Control Systems

Yew-Wen Liang, *Member, IEEE*, Sheng-Dong Xu, *Student Member, IEEE*, and Li-Wei Ting

***Abstract*—This paper studies the robust reliable control issues based on the Takagi–Sugeno (T–S) fuzzy system modeling method and the sliding-mode control (SMC) technique. The combined scheme is shown to have the merits of both approaches. It not only alleviates the online computational burden by using the T–S fuzzy model to implement the original nonlinear system (since most of the system parameters of the T–S model can be offline computed) but also preserves the advantages of the SMC schemes, including rapid response and robustness. Moreover, the combined scheme does not require online computation of any nonlinear term of the original dynamics, and the increase in the partition number of the region of premise variables does not create extra online computational burdens for the scheme. Under the design, the control mission can continue safely without prompt external support, even when some of the actuators fail to operate. Meanwhile, both the active and the passive reliable designs are presented. The proposed analytical results are also applied to the attitude control of a spacecraft. Simulation results demonstrate the benefits of the proposed scheme.**

***Index Terms*—Nonlinear control systems, reliable control, sliding-mode control (SMC), Takagi–Sugeno (T–S) fuzzy model.**

I. Introduction

RECENTLY, the study of reliable (or fault tolerance) control, including fault detection and diagnosis (FDD) issues for performing the active reliable tasks, has attracted considerable attention (see, e.g., [9], [17]–[19], [21], [23], [26], [28], [32]–[34], [36], [37]). In general, repair and maintenance services cannot be provided instantly, which makes reliable control issues of paramount importance. The objective of reliable control is to design an appropriate controller such that the closed-loop system can tolerate abnormal operations of specific control components and retain the overall system stability with acceptable system performance. Within the existing reliable control studies, several approaches have been presented. These approaches include the linear-matrix-inequality-based approach [21], the algebraic Riccatti equation-based approach [32], the coprime factorization approach [33], the Hamilton–Jacobi (HJ)-based approach [17], [34], and the sliding-mode control (SMC)-based approach [9], [18], [19]. Among the aforementioned reliable control studies, only the HJ-based and the SMC-based approaches deal with reliability issues for nonlinear systems. However, because the HJ-based approach was designed under an optimal strategy, its reliable controller is inevitably dependent upon the solution of an associated HJ equation, which is, in general, difficult to solve. Although a power series method [13] may alleviate the difficulty through computer calculation, the solution obtained is only approximate, and the computational load grows quickly when the system is complicated. In contrast, the SMC reliable controllers [18], [19] do not require the solution of any HJ equation, and they retain the advantages of conventional SMC designs. Those advantages include rapid response, easy implementation, and robustness to model uncertainties and/or external disturbances [2]–[4], [6], [7], [9]–[11], [14], [15], [18]–[20], [22], [27], [29], [35].

On the other hand, fuzzy theory has been recognized as one of the most powerful tools for system design, and an enormous number of applications have been created over the past several decades (see, e.g., [1], [4]–[6], [8], [14], [16], [20], [22], [24], [26], [30], [31], [36]). Among them, the so-called Takagi–Sugeno (T–S) fuzzy modeling method [30] has attracted considerable attention because of its particular advantages, which include 1) simplicity of concept; 2) ease of construction; 3) allowance of offline computing most of the system parameters; and 4) being justified as a universal approximator [4], [5], [8], [14], [16], [20], [22], [26], [30], [31]. These benefits make the T–S modeling approach particularly useful, particularly when the nonlinear model is complicated. The basic idea of the T–S approach is first to decompose a nonlinear system into several linear local models according to different cases where the associated linear local models best fit the nonlinear model, and then to aggregate each individual linear model into a single nonlinear model in terms of the membership functions of each model. Although a T–S model may approximate the original nonlinear system well, it creates extra model uncertainties when the T–S model is used to implement the original system. To compensate for the additional uncertainties effectively, a set of schemes that combine the T–S model representation with SMC design were recently proposed (see, e.g., [4], [14], [20], [22]). These combined schemes were shown to be able to alleviate the online computational burden. Since the T–S fuzzy model was utilized to represent the original nonlinear system, they also preserved the advantages of rapid response and robustness of the SMC schemes. In light of the remarkable benefits previously mentioned, this paper will investigate the reliability issues from the combined scheme

Manuscript received September 15, 2008; revised June 18, 2009. First published July 7, 2009; current version published August 12, 2009. This work was supported by the National Science Council, Taiwan, under Grants NSC 95-2623-7-009-007-D, NSC 96-2623-7-009-013-D, NSC 96-2221-E-009-228-, NSC 97-2221-E-009-087, and NSC 97-3114-E-009-002.

Y.-W. Liang and L.-W. Ting are with the Department of Electrical and Control Engineering, National Chiao Tung University, Hsinchu 30010, Taiwan (e-mail: ywliang@cn.nctu.edu.tw).

S.-D. Xu is with the Department of Computer Science, National Chengchi University, Taipei 11605, Taiwan.

Color versions of one or more of the figures in this paper are available online at http://ieeexplore.ieee.org.

Digital Object Identifier 10.1109/TIE.2009.2026384

viewpoint. Meanwhile, both the active and the passive reliable designs will be considered.

The remainder of this paper is organized as follows. Section II states the problem and the main goal of this paper. It is followed by the design of the T–S model-based SMC reliable controllers. The analytical results are then applied in Section IV to the attitude control of a spacecraft. Finally, Section V provides the conclusions.

II. Problem Statement

Consider a class of second-order nonlinear control systems

$$\dot{\mathbf{x}}_1 = \mathbf{x}_2 \tag{1}$$

$$\dot{\mathbf{x}}_2 = \mathbf{f}(\mathbf{x}) + G(\mathbf{x})\mathbf{u} + \mathbf{d}. \tag{2}$$

Here, $\mathbf{x}_1 = (x_1, \ldots, x_n)^{\mathrm{T}} \in \mathbb{R}^n$, $\mathbf{x}_2 = (x_{n+1}, \ldots, x_{2n})^{\mathrm{T}} \in \mathbb{R}^n$ and $\mathbf{x} = (\mathbf{x}_1^{\mathrm{T}}, \mathbf{x}_2^{\mathrm{T}})^{\mathrm{T}}$ are the system states, $\mathbf{u} = (u_1, \ldots, u_m)^{\mathrm{T}} \in \mathbb{R}^m$ with $m > n$ are the control inputs, $\mathbf{d} = (d_1, \ldots, d_n)^{\mathrm{T}} \in \mathbb{R}^n$ denote possible model uncertainties and/or external disturbances, $\mathbf{f}(\mathbf{x}) \in \mathbb{R}^n$ and $G(\mathbf{x}) \in \mathbb{R}^{n\times m}$ are smooth functions with $\mathbf{f}(\mathbf{0}) = \mathbf{0}$, and $(\cdot)^{\mathrm{T}}$ denotes the transpose of a vector or a matrix. Note that, System (1) and (2) has been assumed to have control input redundancy for reliable control task. Define

$$\Phi := \{G_\alpha(\mathbf{x}) | G_\alpha(\mathbf{x}) \text{ is a square matrix formed by taking } n \text{ columns from } G(\mathbf{x})\}. \tag{3}$$

In this paper, we assume that all of the matrices in Φ are *uniformly invertible*, in the sense as stated in Assumption 1 below.

Assumption 1: There exists a positive constant σ_0 such that $\sigma_{\min}(G_\alpha(\mathbf{x})) \geq \sigma_0$ for all $\mathbf{x}$ and for all $G_\alpha(\mathbf{x}) \in \Phi$, where $\sigma_{\min}(\cdot)$ denotes the minimum singular value of a matrix.

In the following, we will investigate the active reliable control issues for System (1) and (2). That is, we assume that the actuators' fault has been successfully detected and diagnosed by an FDD mechanism. The fault may be time varying and include degradation, amplification and outage [18], [28], [36]. Before the occurrence of faults, the engineers may take any kind of control strategy to fulfill their desired system performance. When the fault is detected and diagnosed, the control law is guided to switch to an active reliable law for ensuring system performance. Thus, after the fault is detected, we may divide the actuators into two groups $\mathcal{H}$ and $\mathcal{F}$, within which we assume that all of the actuators in $\mathcal{H}$ are healthy, while those in $\mathcal{F}$ experience faults. This implies that System (1) and (2) can be rewritten as

$$\dot{\mathbf{x}}_1 = \mathbf{x}_2 \tag{4}$$

$$\dot{\mathbf{x}}_2 = \mathbf{f}(\mathbf{x}) + G_{\mathcal{H}}(\mathbf{x})\mathbf{u}_{\mathcal{H}} + G_{\mathcal{F}}(\mathbf{x})\mathbf{u}_{\mathcal{F}} + \mathbf{d} \tag{5}$$

where $G(\mathbf{x}) = (G_{\mathcal{H}}(\mathbf{x})G_{\mathcal{F}}(\mathbf{x}))$. In the rest of this paper, we assume that $\mathbf{u}_{\mathcal{H}} \in \mathbb{R}^k$, $\mathbf{u}_{\mathcal{F}} \in \mathbb{R}^{m-k}$ and $k \geq n$ since the assumption of $\mathrm{rank}(G_{\mathcal{H}}(\mathbf{x})) = n$ is necessary for the existence of equivalent control in SMC design [10].

The objective of this paper is then to organize an appropriate $\mathbf{u}_{\mathcal{H}}$ so that the origin of the closed-loop system is asymptotically stable even when the actuators in $\mathcal{F}$ are detected and diagnosed as experiencing faults by an FDD mechanism.

We recall the following lemma which is needed in the succeeding derivations.

Lemma 1: Let Q_1, $Q_2 \in \mathbb{R}^{n\times m}$ be two matrices with $\mathrm{rank}(Q_1) = n$ [12]. Then,

(i) $\|Q_1\| = \sigma_{\max}(Q_1)$

(ii) $\left\|Q_1^+\right\| = \left\|Q_1^{\mathrm{T}}\left(Q_1 Q_1^{\mathrm{T}}\right)^{-1}\right\| = 1/\sigma_{\min}(Q_1)$

(iii) $\sigma_{\min}(Q_1 + Q_2) \geq \sigma_{\min}(Q_1) - \sigma_{\max}(Q_2)$

where $\|\cdot\|$, $(\cdot)^+$, and $\sigma_{\max}(\cdot)$ denote the Euclidean norm, the pseudoinverse, and the maximum singular value of a matrix, respectively.

III. T–S Model-Based SMC Reliable Design

In light of the advantages of the T–S modeling and SMC approaches as stated above, this paper will combine the two schemes for the design of reliable controllers.

A. T–S Fuzzy Model Description

It is known that a nonlinear system can be approximated by a T–S fuzzy model [22], [30], which is described by a combination of several linear models with suitable weighting. The ith $(i = 1, 2, \ldots, p)$ rule of the T–S fuzzy model for System (4) and (5) has the following form.

If ζ_1 is $M_{1_i}, \ldots, \zeta_q$ is M_{q_i}, $i = 1, \ldots, p$, then

$$\dot{\mathbf{x}}_1 = \mathbf{x}_2 \tag{6}$$

$$\dot{\mathbf{x}}_2 = A_i\mathbf{x} + B_{\mathcal{H}i}\mathbf{u}_{\mathcal{H}} + B_{\mathcal{F}i}\mathbf{u}_{\mathcal{F}} \tag{7}$$

where $\zeta_1, \ldots, \zeta_q$ are premise variables, $M_{1_i}, \ldots, M_{q_i}$ are membership functions for premise variables, p and q denote the number of rules and premise variables, $A_i \in \mathbb{R}^{n\times n}$, $B_{\mathcal{H}i} \in \mathbb{R}^{n\times k}$, and $B_{\mathcal{F}i} \in \mathbb{R}^{n\times(m-k)}$, $k \geq n$. The T–S fuzzy model is then constructed according to the weight of system state on each linear model as (8) and (9) below

$$\dot{\mathbf{x}}_1 = \mathbf{x}_2 \tag{8}$$

$$\dot{\mathbf{x}}_2 = A(\mathbf{x}) + B_{\mathcal{H}}(\mathbf{x})\mathbf{u}_{\mathcal{H}} + B_{\mathcal{F}}(\mathbf{x})\mathbf{u}_{\mathcal{F}} \tag{9}$$

where $A(\mathbf{x}) := \sum_{i=1}^p \alpha_i(\mathbf{x})A_i\mathbf{x}$, $B_{\mathcal{H}}(\mathbf{x}) := \sum_{i=1}^p \alpha_i(\mathbf{x})B_{\mathcal{H}}i$, $B_{\mathcal{F}}(\mathbf{x}) := \sum_{i=1}^p \alpha_i(\mathbf{x})B_{\mathcal{F}}i$, and the weightings $\alpha_i(\mathbf{x}) \geq 0$ for all i and $\sum_{i=1}^p \alpha_i(\mathbf{x}) = 1$.

B. SMC Reliable Design

By incorporating the T–S fuzzy model description, System (4) and (5) can be rewritten as

$$\dot{\mathbf{x}}_1 = \mathbf{x}_2 \tag{10}$$

$$\dot{\mathbf{x}}_2 = A(\mathbf{x}) + \Delta\mathbf{f} + (B_{\mathcal{H}}(\mathbf{x}) + \Delta G_{\mathcal{H}})\,\mathbf{u}_{\mathcal{H}} + (B_{\mathcal{F}}(\mathbf{x}) + \Delta G_{\mathcal{F}})\,\mathbf{u}_{\mathcal{F}} + \mathbf{d} \tag{11}$$

where $\Delta\mathbf{f} := \mathbf{f}(\mathbf{x}) - A(\mathbf{x})$, $\Delta G_{\mathcal{H}} := G_{\mathcal{H}}(\mathbf{x}) - B_{\mathcal{H}}(\mathbf{x})$, and $\Delta G_{\mathcal{F}} := G_{\mathcal{F}}(\mathbf{x}) - B_{\mathcal{F}}(\mathbf{x})$. Since a smooth nonlinear

dynamical system can be accurately approximated by a T–S model if enough fuzzy rules are used (see, e.g., [31]), we impose the following assumption concerning the error of the control input matrices between the original and the T–S models.

Assumption 2: There exists a positive constant σ, $\sigma < \sigma_0/2$, such that $\|\Delta G\| < \sigma$, where $\Delta G = (\Delta G_{\mathcal{H}} \Delta G_{\mathcal{F}})$ and σ_0 is defined in Assumption 1.

Note that, ΔG is a function of $\mathbf{x}$, $\sigma_{\max}(\Delta G_{\mathcal{H}}) = \|\Delta G_{\mathcal{H}}\| \leq \|\Delta G\| < \sigma$ by Assumption 2, and $\sigma_{\min}(G_{\mathcal{H}}(\mathbf{x})) \geq \sigma_0$ by Assumption 1. It follows from Lemma 1 that $\sigma_{\min}(B_{\mathcal{H}}(\mathbf{x})) = \sigma_{\min}(G_{\mathcal{H}}(\mathbf{x}) - \Delta G_{\mathcal{H}}) \geq \sigma_{\min}(G_{\mathcal{H}}(\mathbf{x})) - \sigma_{\max}(\Delta G_{\mathcal{H}}) \geq \sigma_0 - \sigma > \sigma_0/2$. Thus, $\text{rank}(B_{\mathcal{H}}(\mathbf{x})) = n$ for all $\mathbf{x}$. In addition, we assume that the control inputs in the set of $\mathcal{F}$ are diagnosed as

$$\mathbf{u}_{\mathcal{F}} = \hat{\mathbf{u}}_{\mathcal{F}} + \Delta \mathbf{u}_{\mathcal{F}} \tag{12}$$

where $\hat{\mathbf{u}}_{\mathcal{F}}$ and $\Delta \mathbf{u}_{\mathcal{F}}$ denote the estimated control value and estimated error, respectively. The estimated error $\Delta \mathbf{u}_{\mathcal{F}}$ is treated as an additional uncertainty that should be compensated.

Since System (10) and (11) is a set of second-order systems, we may assume the sliding surface in the form of

$$\mathbf{s} := \mathbf{x}_2 + M\mathbf{x}_1 \tag{13}$$

where $M \in \mathbb{R}^{n \times n}$ is a positive definite matrix. Clearly, if the system state remains on the sliding surface, then the desired stabilization performance of $\mathbf{x}(t) \to \mathbf{0}$ can be exponentially achieved with a convergence rate depending on the choice of the eigenvalues of M [10], [20]. From (10), (11), and (13), we have

$$\begin{aligned}\dot{\mathbf{s}} = M\mathbf{x}_2 + A(\mathbf{x}) + \Delta \mathbf{f} + (B_{\mathcal{H}}(\mathbf{x}) + \Delta G_{\mathcal{H}})\, \mathbf{u}_{\mathcal{H}} \\ + (B_{\mathcal{F}}(\mathbf{x}) + \Delta G_{\mathcal{F}})\, (\hat{\mathbf{u}}_{\mathcal{F}} + \Delta \mathbf{u}_{\mathcal{F}}) + \mathbf{d}.\end{aligned} \tag{14}$$

According to the SMC design procedure [10], [20], we choose

$$\mathbf{u}_{\mathcal{H}} = \mathbf{u}_{\mathcal{H}}^{eq} + \mathbf{u}_{\mathcal{H}}^{re} \tag{15}$$

$$\mathbf{u}_{\mathcal{H}}^{eq} = -B_{\mathcal{H}}^{+}(\mathbf{x}) \cdot (M\mathbf{x}_2 + A(\mathbf{x}) + B_{\mathcal{F}}(\mathbf{x})\hat{\mathbf{u}}_{\mathcal{F}}) \tag{16}$$

where

$$B_{\mathcal{H}}^{+}(\mathbf{x}) := B_{\mathcal{H}}^{\mathrm{T}}(\mathbf{x}) \cdot \left(B_{\mathcal{H}}(\mathbf{x}) B_{\mathcal{H}}^{\mathrm{T}}(\mathbf{x})\right)^{-1}. \tag{17}$$

Note that $\mathbf{u}_{\mathcal{H}}^{eq}$, given by (16), involves the information of diagnosis. From (14)–(16), we have

$$\dot{\mathbf{s}} = \Delta_m + (B_{\mathcal{H}}(\mathbf{x}) + \Delta G_{\mathcal{H}})\, \mathbf{u}_{\mathcal{H}}^{re} \tag{18}$$

where

$$\begin{aligned}\Delta_m = \Delta \mathbf{f} + \Delta G_{\mathcal{H}} \mathbf{u}_{\mathcal{H}}^{eq} + B_{\mathcal{F}}(\mathbf{x}) \Delta \mathbf{u}_{\mathcal{F}} \\ + \Delta G_{\mathcal{F}}(\hat{\mathbf{u}}_{\mathcal{F}} + \Delta \mathbf{u}_{\mathcal{F}}) + \mathbf{d}.\end{aligned} \tag{19}$$

As previously mentioned, the difference between the T–S and the original models may be assumed to be small, and the fault is successfully diagnosed. Thus, $\|\Delta \mathbf{f}\|$, $\|\Delta G_{\mathcal{H}}\|$, $\|\Delta G_{\mathcal{F}}\|$ and $\|\Delta \mathbf{u}_{\mathcal{F}}\|$ are small, and hence Δ_m is bounded, provided that $\mathbf{d}$ is bounded. We impose the following assumption.

Assumption 3: There exists a nonnegative scalar function $\rho(\mathbf{x}, t)$ such that $\|\Delta_m\| \leq \rho(\mathbf{x}, t)$.

Note that, although the inequality given in Assumption 3 requires the information of $\mathbf{u}_{\mathcal{H}}^{eq}$, $\rho(\mathbf{x}, t)$ can be easily obtained after the calculation of $\mathbf{u}_{\mathcal{H}}^{eq}$ since the upper bounds of $\|\Delta \mathbf{f}\|$ and $\|\Delta G\|$ can be offline estimated. Following the SMC design procedure, we select

$$\mathbf{u}_{\mathcal{H}}^{re} = -\mu \cdot B_{\mathcal{H}}^{+}(\mathbf{x}) \cdot \text{sgn}(\mathbf{s}), \quad \mu \geq \frac{\sigma_0 - \sigma}{\sigma_0 - 2\sigma}\left(\eta + \rho(\mathbf{x}, t)\right) \tag{20}$$

where $\text{sgn}(\mathbf{s}) = (\text{sgn}(s_1), \ldots, \text{sgn}(s_n))^{\mathrm{T}}$ and $\eta > 0$ which affects the convergence speed of the system state to the sliding surface. We have the following result.

Theorem 1: Suppose that System (1) and (2) experiences actuator faults at control channels denoted by $\mathcal{F}$ with estimated control values $\hat{\mathbf{u}}_{\mathcal{F}}$ and estimated errors $\Delta \mathbf{u}_{\mathcal{F}}$ as given by (12). If, in addition, the T–S model-based errors given by (10) and (11), the actuator faults and the system parameters satisfy Assumptions 1–3, then the origin of System (1) and (2) is asymptotically stable under the control laws given by (15), (16), (20).

Proof: Since $B_{\mathcal{H}}(\mathbf{x}) = G_{\mathcal{H}}(\mathbf{x}) - \Delta G_{\mathcal{H}}$, we have from Lemma 1 that

$$\begin{aligned}\left\|B_{\mathcal{H}}^{+}(\mathbf{x})\right\| &= \left\|(G_{\mathcal{H}}(\mathbf{x}) - \Delta G_{\mathcal{H}})^{+}\right\| \\ &= \frac{1}{\sigma_{\min}\left(G_{\mathcal{H}}(\mathbf{x}) - \Delta G_{\mathcal{H}}\right)} \\ &\leq \frac{1}{\sigma_{\min}\left(G_{\mathcal{H}}(\mathbf{x})\right) - \sigma_{\max}(\Delta G_{\mathcal{H}})}.\end{aligned}$$

Note that, $\sigma_{\min}(G_{\mathcal{H}}(\mathbf{x})) \geq \min_{G_\alpha(\mathbf{x}) \in \Phi}\{\sigma_{\min}(G_\alpha(\mathbf{x}))\} \geq \sigma_0$ by Assumption 1, and $\sigma_{\max}(\Delta G_{\mathcal{H}}) = \|\Delta G_{\mathcal{H}}\| \leq \|\Delta G\| < \sigma$ by Assumption 2. It follows that

$$\left\|B_{\mathcal{H}}^{+}(\mathbf{x})\right\| \leq \frac{1}{\sigma_0 - \sigma}. \tag{21}$$

Moreover, from (18) and (19), Assumptions 2 and 3, and the fact that $\|\Delta G_{\mathcal{H}}\| \leq \|\Delta G\| < \sigma$, we have

$$\begin{aligned}\mathbf{s}^{\mathrm{T}}\dot{\mathbf{s}} &= \mathbf{s}^{\mathrm{T}}\Delta_m + \mathbf{s}^{\mathrm{T}} B_{\mathcal{H}}(\mathbf{x}) \mathbf{u}_{\mathcal{H}}^{re} + \mathbf{s}^{\mathrm{T}} \Delta G_{\mathcal{H}} \mathbf{u}_{\mathcal{H}}^{re} \\ &\leq \rho(\mathbf{x}, t)\|\mathbf{s}\| - \mu \mathbf{s}^{\mathrm{T}} \text{sgn}(\mathbf{s}) + \mu\sigma\|\mathbf{s}\| \cdot \left\|B_{\mathcal{H}}^{+}(\mathbf{x}) \cdot \text{sgn}(\mathbf{s})\right\|.\end{aligned} \tag{22}$$

Since $\mathbf{s}^{\mathrm{T}}\text{sgn}(\mathbf{s}) = \sum_{i=1}^{n} |s_i| \geq \|\mathbf{s}\|$ and $\|B_{\mathcal{H}}^{+}(\mathbf{x}) \cdot \text{sgn}(\mathbf{s})\| = \|B_{\mathcal{H}}^{+}(\mathbf{x})\|$, it follows from (20)–(22) that

$$\begin{aligned}\mathbf{s}^{\mathrm{T}}\dot{\mathbf{s}} &\leq \left(\rho(\mathbf{x}, t) - \mu + \frac{\mu\sigma}{\sigma_0 - \sigma}\right) \cdot \|\mathbf{s}\| \\ &\leq -\eta \cdot \|\mathbf{s}\|.\end{aligned} \tag{23}$$

Thus, the system state will reach the sliding surface in a finite amount of time, and the reaching speed depends on the magnitude of η [10]. Hence, the conclusion of the theorem

follows, since the origin of the reduced-order dynamics $\dot{x}_1 = -Mx_1$ given in (13) is also asymptotically stable. ■

Remark 1: Although the derivations, as stated above, are mainly for active reliable strategies which require FDD information and controllers reconfiguration when faults happen, they can be easily extended to passive reliable schemes which need not to reconfigure the controllers but needs to prespecify a set of susceptible actuators $\mathcal{F}$ as many as possible (i.e., $k = n$) so that the system remains stable even when all of the selected susceptible actuators fail to operate [19]. Statistical information regarding the failure rate of each actuator would be helpful for selecting the two sets $\mathcal{F}$ and $\mathcal{H}$. After the two set of actuators $\mathcal{F}$ and $\mathcal{H}$ are chosen for passive reliable purpose, Assumptions 1 and 2 are modified to be $\sigma_{\min}(G_{\mathcal{H}}(\mathbf{x})) \geq \sigma_0$ and $\|\Delta G_{\mathcal{H}}\| < \sigma < \sigma_0/2$, respectively. The passive reliable control law is then adjusted as

$$\mathbf{u}_{\mathcal{H}} = -B_{\mathcal{H}}^{-1}(\mathbf{x}) \cdot (M\mathbf{x}_2 + A(\mathbf{x}) + \mu \cdot \operatorname{sgn}(\mathbf{s})) \quad (24)$$

$$\text{with} \quad \mu \geq \frac{\sigma_0 - \sigma}{\sigma_0 - 2\sigma}\left(\eta + \rho_p(\mathbf{x}, t)\right). \quad (25)$$

Here, $\rho_p(\mathbf{x}, t)$ is an upper bound of $\|\Delta\mathbf{f} + \Delta G_{\mathcal{H}}\mathbf{u}_{\mathcal{H}}^{eq} + G_{\mathcal{F}}(\mathbf{x})\mathbf{u}_{\mathcal{F}}^{*} + \mathbf{d}\|$ and $\mathbf{u}_{\mathcal{F}}^{*}$ denotes the actual faulty value which might locate at any place inside the possible range of $\mathbf{u}_{\mathcal{F}}$. Clearly, the passive reliable controller (24) and (25) does not involve any FDD information. Nevertheless, since the passive reliable schemes have to account for all possible faulty values produced by the actuators in $\mathcal{F}$, the upper bound $\rho_p(\mathbf{x}, t)$ for passive reliable designs are, in general, much larger than the upper bound $\rho(\mathbf{x}, t)$ for active version particularly when the FDD estimation is accurate (i.e., $\Delta\mathbf{u}_{\mathcal{F}}$ is small enough). Aside from when some or all of the actuators in $\mathcal{F}$ are healthy, one may choose

$$\mathbf{u}_{\mathcal{F}} = -\nu \cdot \operatorname{sgn}\left(B_{\mathcal{F}}^{\mathrm{T}}(\mathbf{x}) \cdot \mathbf{s}\right), \quad \nu > 0 \quad (26)$$

instead of $\mathbf{u}_{\mathcal{F}} = \mathbf{0}$ to speed up the convergent performance of the system state to the selected sliding surface [19].

Remark 2: Suppose that the control input matrix $G(\mathbf{x})$ does not vary, i.e., $G(\mathbf{x}) \equiv G = (G_{\mathcal{H}}G_{\mathcal{F}})$ is a constant matrix. Then, Assumption 1 is satisfied if any n columns taken from G are linearly independent. The control input matrices $B_{\mathcal{H}}(\mathbf{x})$ and $B_{\mathcal{F}}(\mathbf{x})$ of the T–S model are then identical to $G_{\mathcal{H}}$ and $G_{\mathcal{F}}$, respectively. It implies that $\|\Delta G\| = 0$ in Assumption 2. Thus, the overall active reliable asymptotic stabilizers, as stated in (15), (16), and (20), are modified as

$$\mathbf{u}_{\mathcal{H}} = -G_{\mathcal{H}}^{+} \cdot (M\mathbf{x}_2 + A(\mathbf{x}) + G_{\mathcal{F}}\hat{\mathbf{u}}_{\mathcal{F}} + \mu \cdot \operatorname{sgn}(\mathbf{s})) \quad (27)$$

where $\mu \geq \eta + \rho(\mathbf{x}, t)$ and $\rho(\mathbf{x}, t)$ is an upper bound of $\|\Delta_m\| := \|\Delta\mathbf{f} + G_{\mathcal{F}}\Delta\mathbf{u}_{\mathcal{F}} + \mathbf{d}\|$. Similarly, the passive reliable laws (24)–(26) are changed to be

$$\mathbf{u}_{\mathcal{H}} = -G_{\mathcal{H}}^{-1} \cdot (M\mathbf{x}_2 + A(\mathbf{x}) + \mu \cdot \operatorname{sgn}(\mathbf{s})) \quad (28)$$

$$\mathbf{u}_{\mathcal{F}} = -\nu \cdot \operatorname{sgn}\left(G_{\mathcal{F}}^{\mathrm{T}} \cdot \mathbf{s}\right). \quad (29)$$

Here, $\mu \geq \eta + \rho_p(\mathbf{x}, t)$, $\eta > 0$, $\rho_p(\mathbf{x}, t)$ is an upper bound of $\|\Delta\mathbf{f} + G_{\mathcal{F}}(\mathbf{x})\mathbf{u}_{\mathcal{F}}^{*} + \mathbf{d}\|$, where $\mathbf{u}_{\mathcal{F}}^{*}$ denotes the possible faulty values of the actuators in $\mathcal{F}$ and $\nu > 0$.

Remark 3: The parallel distributed compensation (PDC) controller is known to have the form $\mathbf{u} = -\sum_{i=1}^{p} \alpha_i(\mathbf{x})K_i\mathbf{x}$, where K_i is the constant linear feedback gain associated with the ith rule [31]. According to the structure, the equivalent controller (16) for the active design may be easily rearranged in a similar form as $\mathbf{u}_{\mathcal{H}}^{eq} = -B_{\mathcal{H}}^{+}(\mathbf{x}) \cdot \sum_{i=1}^{p} \alpha(\mathbf{x})[E_i\mathbf{x} + B_{\mathcal{F}i}(\mathbf{x})\hat{\mathbf{u}}_{\mathcal{F}}]$, where $E_i = (0M) + A_i$ and $E_i\mathbf{x} = M\mathbf{x}_2 + A_i\mathbf{x}$. When the control input matrix $G(\mathbf{x})$ is constant, the matrix $B_{\mathcal{H}}^{+}(\mathbf{x})$ given by (17) is also a constant matrix, denoted by $B_{\mathcal{H}}^{+}$. It follows that the equivalent controller becomes a PDC controller with $K_i = B_{\mathcal{H}}^{+} \cdot E_i$, together with an additional term that involves the fault information. Similarly, the equivalent controller for the passive design can also be put in the same structures as those of active version without the term that includes the fault information.

IV. Application to Spacecraft Attitude Stabilization

An attitude model for a spacecraft along a circular orbit can be described in the same form as (1) and (2) with $n = 3$ [19]. The three Euler's angles (ϕ, θ, ψ) and their derivatives are adopted as the six state variables. For simplicity, we assume in this paper that the thruster is the only applied control force and there is an actuator redundancy for the reliable task. By letting $\mathbf{x} = (\phi, \theta, \psi, \dot{\phi}, \dot{\theta}, \dot{\psi})^{\mathrm{T}}$ and $\mathbf{f}(\mathbf{x}) = (f_1(\mathbf{x}), f_2(\mathbf{x}), f_3(\mathbf{x}))^{\mathrm{T}}$, the overall system dynamics has parameters described as below

$$\begin{aligned} f_1(\mathbf{x}) =& \omega_0 x_6 c x_3 c x_2 - \omega_0 x_5 s x_3 s x_2 \\ &+ \frac{I_y - I_z}{I_x}\Big[x_5 x_6 + \omega_0 x_5 c x_1 s x_3 s x_2 + \omega_0 x_5 c x_3 s x_1 \\ &\quad + \omega_0 x_6 c x_3 c x_1 + \frac{1}{2}\omega_0^2 s(2x_3) c^2 x_1 s x_2 \\ &\quad + \frac{1}{2} w_0^2 c^2 x_3 s(2x_1) - \omega_0 x_6 s x_3 s x_2 s x_1 \\ &\quad - \frac{1}{2}\omega_0^2 s^2 x_2 s^2 x_3 s(2x_1) \\ &\quad - \frac{1}{2}\omega_0^2 s(2x_3) s x_2 s^2 x_1 \\ &\quad - \frac{3}{2}\omega_0^2 c^2 x_2 s(2x_1)\Big] \end{aligned} \quad (30)$$

$$\begin{aligned} f_2(\mathbf{x}) =& \omega_0 x_6 s x_3 c x_1 + \omega_0 x_4 c x_3 s x_1 + \omega_0 x_6 c x_3 s x_2 s x_1 \\ &+ \omega_0 x_5 s x_3 c x_2 s x_1 + \omega_0 x_4 s x_3 s x_2 c x_1 \\ &+ \frac{I_z - I_x}{I_y}\Big[x_4 x_6 + \omega_0 x_4 c x_1 s x_3 s x_2 \\ &\quad + \omega_0 x_4 c x_3 s x_1 - \omega_0 x_6 s x_3 c x_2 \\ &\quad - \frac{1}{2}\omega_0^2 s(2x_2) s^2 x_3 c x_1 \\ &\quad - \frac{1}{2} w_0^2 c x_2 s x_1 s(2x_3) \\ &\quad + \frac{3}{2}\omega_0^2 s(2x_2) c x_1\Big] \end{aligned} \quad (31)$$

$$
\begin{aligned}
f_3(\mathbf{x}) =& \omega_0 x_4 s x_1 s x_3 s x_2 - \omega_0 x_6 c x_1 c x_3 s x_2 \\
&- \omega_0 x_5 c x_1 s x_3 c x_2 + \omega_0 x_6 s x_3 s x_1 - \omega_0 x_4 c x_3 c x_1 \\
&+ \frac{I_x - I_y}{I_z}\Bigg[x_4 x_5 + \omega_0 x_4 c x_3 c x_1 \\
&\qquad - \omega_0 x_4 s x_3 s x_2 s x_1 - \omega_0 x_5 s x_3 c x_2 \\
&\qquad - \frac{1}{2}\omega_0^2 s(2x_3) c x_2 c x_1 \\
&\qquad + \frac{1}{2} w_0^2 s^2 x_3 s x_1 s(2x_2) \\
&\qquad - \frac{3}{2}\omega_0^2 s(2x_2) s x_1\Bigg] \qquad (32)
\end{aligned}
$$

$$
G(\mathbf{x}) = G = \begin{pmatrix} 0.67 & 0.67 & 0.67 & 0.67 \\ 0.69 & -0.69 & -0.69 & 0.69 \\ 0.28 & 0.28 & -0.28 & -0.28 \end{pmatrix}. \qquad (33)
$$

Here, I_x, I_y, and I_z are the inertia with respect to the three body coordinate axes, ω_0 denotes the constant orbital rate, and c and s denote the cos and sin functions, respectively. Note that, the system is controllable for any three of the control inputs being healthy, and we have an additional control channel for reliable control task.

To derive an appropriate T–S model to approximate the original nonlinear dynamics, we first express $\mathbf{f}(\mathbf{x}) = F(\mathbf{x})\mathbf{x}$. A set of entries of $F(\mathbf{x})$ have the following forms:

$$
\begin{aligned}
(F(\mathbf{x}))_{1,1} =& \frac{I_y - I_z}{I_x}\Bigg[w_0^2 c^2 x_3 \frac{s(2x_1)}{2x_1} \\
&- \omega_0^2 s^2 x_2 s^2 x_3 \frac{s(2x_1)}{2x_1} \\
&- 3\omega_0^2 c^2 x_2 \frac{s(2x_1)}{2x_1}\Bigg] \\
(F(\mathbf{x}))_{1,2} =& \frac{I_y - I_z}{I_x}\Bigg[\frac{1}{4}\omega_0^2 s(2x_3) c^2 x_1 \frac{s x_2}{x_2} \\
&- \frac{1}{4}\omega_0^2 s(2x_3) \frac{s x_2}{x_2} s^2 x_1\Bigg] \\
(F(\mathbf{x}))_{1,3} =& \frac{I_y - I_z}{I_x}\Bigg[\frac{1}{2}\omega_0^2 \frac{s(2x_3)}{2x_3} c^2 x_1 s x_2 \\
&- \frac{1}{2}\omega_0^2 \frac{s(2x_3)}{2x_3} s x_2 s^2 x_1\Bigg] \\
(F(\mathbf{x}))_{1,4} =& 0 \\
(F(\mathbf{x}))_{1,5} =& -\omega_0 s x_3 s x_2 + \frac{I_y - I_z}{I_x} \\
&\cdot \left[\frac{1}{2} x_6 + \omega_0 c x_1 s x_3 s x_2 + \omega_0 c x_3 s x_1\right] \\
(F(\mathbf{x}))_{1,6} =& \omega_0 c x_3 c x_2 \\
&+ \frac{I_y - I_z}{I_x}\left[\frac{1}{2} x_5 + \omega_0 c x_3 c x_1 - \omega_0 s x_3 s x_2 s x_1\right] \\
(F(\mathbf{x}))_{2,1} =& \frac{I_z - I_x}{I_y}\left[-\frac{1}{4} w_0^2 c x_2 \frac{s x_1}{x_1} s(2x_3)\right] \\
(F(\mathbf{x}))_{2,2} =& \frac{I_z - I_x}{I_y}\Bigg[-\omega_0^2 \frac{s(2x_2)}{2x_2} s^2 x_3 c x_1 \\
&+ 3\omega_0^2 \frac{s(2x_2)}{2x_2} c x_1\Bigg] \\
(F(\mathbf{x}))_{2,3} =& \frac{I_z - I_x}{I_y}\left[-\frac{1}{2} w_0^2 c x_2 s x_1 \frac{s(2x_3)}{2x_3}\right] \\
(F(\mathbf{x}))_{2,4} =& \omega_0 c x_3 s x_1 + \omega_0 s x_3 s x_2 c x_1 + \frac{I_z - I_x}{I_y} \\
&\cdot \left[\frac{1}{2} x_6 + \omega_0 c x_1 s x_3 s x_2 + \omega_0 c x_3 s x_1\right] \\
(F(\mathbf{x}))_{2,5} =& \omega_0 s x_3 c x_2 s x_1 \\
(F(\mathbf{x}))_{2,6} =& \omega_0 s x_3 c x_1 + \omega_0 c x_3 s x_2 s x_1 \\
&+ \frac{I_z - I_x}{I_y}\left[\frac{1}{2} x_4 - \omega_0 s x_3 c x_2\right] \\
(F(\mathbf{x}))_{3,1} =& \frac{I_x - I_y}{I_z}\left[-\frac{3}{4}\omega_0^2 s(2x_2) \frac{s x_1}{x_1}\right] \\
(F(\mathbf{x}))_{3,2} =& \frac{I_x - I_y}{I_z}\Bigg[w_0^2 s^2 x_3 s x_1 \frac{s(2x_2)}{2x_2} \\
&- \frac{3}{2}\omega_0^2 \frac{s(2x_2)}{2x_2} s x_1\Bigg] \\
(F(\mathbf{x}))_{3,3} =& \frac{I_x - I_y}{I_z}\left[-\omega_0^2 \frac{s(2x_3)}{2x_3} c x_2 c x_1\right] \\
(F(\mathbf{x}))_{3,4} =& \omega_0 s x_1 s x_3 s x_2 - \omega_0 c x_3 c x_1 + \frac{I_x - I_y}{I_z} \\
&\cdot \left[\frac{1}{2} x_5 + \omega_0 c x_3 c x_1 - \omega_0 s x_3 s x_2 s x_1\right] \\
(F(\mathbf{x}))_{3,5} =& -\omega_0 c x_1 s x_3 c x_2 \\
&+ \frac{I_x - I_y}{I_z}\left[\frac{1}{2} x_4 - \omega_0 s x_3 c x_2\right] \\
(F(\mathbf{x}))_{3,6} =& -\omega_0 c x_1 c x_3 s x_2 + \omega_0 s x_3 s x_1
\end{aligned}
$$

where $(F(\mathbf{x}))_{i,j}$ denotes the (i,j)-entry of the matrix $F(\mathbf{x})$. Next, a set of operating points will be selected for the construction of the associated linear models. These operating points are selected from the possible workspace, so that the motion of the spacecraft can be well approximated by using a convex combination of the associated linear models. For demonstration, we assume that $I_x = I_z = 2000\ \mathrm{N \cdot m \cdot s^2}$, $I_y = 400\ \mathrm{N \cdot m \cdot s^2}$, $\omega_0 = 1.0312 \times 10^{-3}$ rad/s, and the angular positions are constrained to be x_1, $x_3 \in [-\pi, \pi]$ and $x_2 \in [-\pi/2, \pi/2]$. Since the modern control systems are constructed more and more complicated, the employed control strategy and the time required for controller implementation have inevitably become extremely important, which greatly influence the success, the efficiency and the reliability of a control task. To investigate the effects of the number of premise variables on system performances, we consider the following two cases: the first takes the three angles as premise variables, while the second includes all of the six state variables.

A. Case for Three Premise Variables

In this case, the operating points are chosen in the form of $\{\mathbf{x}_{i,j,k} = (x_{1,i}, x_{2,j}, x_{3,k}, 0, 0, 0)^{\mathrm{T}} | i = 1, \ldots, n_1, j = 1, \ldots, n_2, k = 1, \ldots, n_3\}$, where $\{x_{1,1}, \ldots, x_{1,n_1}\}$,

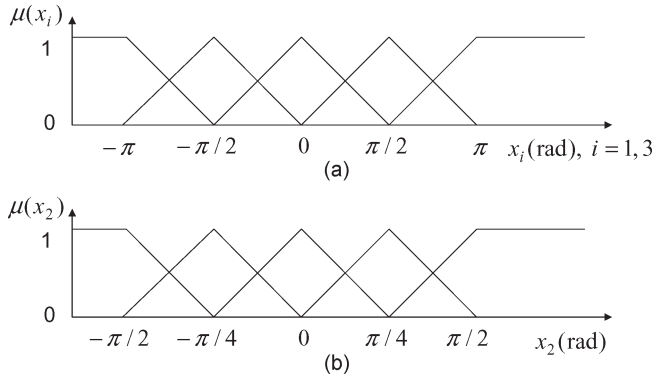

Fig. 1. Membership functions for the states x_1, x_2, and x_3 in Case A.

$\{x_{2,1}, \ldots, x_{2,n_2}\}$ and $\{x_{3,1}, \ldots, x_{3,n_3}\}$ are three selected partitions of $[-\pi, \pi]$, $[-\pi/2, \pi/2]$, and $[-\pi, \pi]$, respectively. In this case, we select $n_1 = n_2 = n_3 = 5$ and employ the triangular membership functions, as shown in Fig. 1. Under these settings, we have $5^3 = 125$ operating points. The associated 125 linear local models can then be easily obtained. Three of them are listed as below

$$A_{1,1,1} = 10^{-6} \cdot \begin{pmatrix} 0 & 0 & 0 & 0 & 0 & -824.96 \\ 0 & 0 & 0 & 0 & 0 & 0 \\ 0 & 0 & 0 & -206.24 & 0 & 1031.2 \end{pmatrix}$$

$$A_{2,2,2} = 10^{-6} \cdot \begin{pmatrix} 0 & 0 & 0 & 0 & 729.17 & -583.33 \\ 0 & 0 & 0 & 0 & 729.17 & 0 \\ 0.41 & 0.27 & 0 & -145.83 & 583.33 & 1031.2 \end{pmatrix}$$

$$A_{2,2,4} = 10^{-6} \cdot \begin{pmatrix} 0 & 0 & 0 & 0 & -729.17 & 583.33 \\ 0 & 0 & 0 & 0 & -729.17 & 0 \\ 0.41 & 0.27 & 0 & 145.83 & -583.33 & -1031.2 \end{pmatrix}$$

where $A_{i,j,k} = F(\mathbf{x}_{i,j,k})$ and $\mathbf{f}(\mathbf{x}_{i,j,k}) = A_{i,j,k}\mathbf{x}_{i,j,k}$ for all $1 \le i \le n_1$, $1 \le j \le n_2$ and $1 \le k \le n_3$. After determining the 125 linear local models, we define the region $D_{i,j,k} := \{\mathbf{x} | x_{1,i} \le x_1 \le x_{1,i+1}, x_{2,j} \le x_2 \le x_{2,j+1}, x_{3,k} \le x_3 \le x_{3,k+1}, -1 \le x_l \le 1, l = 4, 5, 6\}$. Then, the T–S fuzzy system model can be easily determined according to $\mathbf{x} \in D_{i,j,k}$ and the adopted triangular membership functions as

$$A(\mathbf{x}) = \sum_{l,m,n=0}^{1} \alpha_l(\mathbf{x})\alpha_m(\mathbf{x})\alpha_n(\mathbf{x}) \cdot A_{i+l,j+m,k+n}\mathbf{x}$$
$$B(\mathbf{x}) = G$$

where $\alpha_l(\mathbf{x}) = |(x_1 - x_{1,i+1-l})/(x_{1,i+1} - x_{1,i})|$, $\alpha_m(\mathbf{x}) = |(x_2 - x_{2,j+1-m})/(x_{2,j+1} - x_{2,j})|$ and $\alpha_n(\mathbf{x}) = |(x_3 - x_{3,k+1-n})/(x_{3,k+1} - x_{3,k})|$. Clearly, $\sum_{l,m,n=0}^{1} \alpha_l(\mathbf{x})\alpha_m(\mathbf{x})\alpha_n(\mathbf{x}) = 1$. The upper bound of $\|\Delta\mathbf{f}\| = \|\mathbf{f}(\mathbf{x}) - A(\mathbf{x})\|$, denoted by $\|\Delta\mathbf{f}\|_\infty$, over the region $D_{i,j,k}$ can then be offline computed. With the aid of MATLAB code [25], these upper bounds are easily determined, as described in Table I. Since the T–S-type controller only uses three premise variables with triangular membership functions, it therefore triggers at most eight rules (i.e., at most 2^3 linear local models) at each time instant. Thus, it does not create an extra online computational burden if the partition for the regions of x_1, x_2, and x_3 are made finer. However, since the maximum value of a function over a smaller subregion is smaller than or equal to that of the same function over the whole region, it follows that a finer partition for the region of x_1, x_2, and x_3 will result in a smaller magnitude of $\rho(\mathbf{x}, t)$ as stated in Assumption 3, or $\rho_p(\mathbf{x}, t)$ in Remark 1 for passive design. Thus, the control magnitude will be smaller if the partition of x_1, x_2, and x_3 are made finer.

TABLE I
ESTIMATED UPPER BOUNDS $\|\Delta\mathbf{f}\|_\infty$ IN THE REGION $D_{i,j,k}$ FOR CASE A

Region	$D_{1,1,1}$	$D_{1,1,2}$	$D_{1,1,3}$	$D_{1,1,4}$	$D_{1,2,1}$	$D_{1,2,2}$
$\|\Delta\mathbf{f}\|_\infty$	1.1329	1.1322	1.1299	1.1304	1.1325	1.1318
Region	$D_{1,2,3}$	$D_{1,2,4}$	$D_{1,3,1}$	$D_{1,3,2}$	$D_{1,3,3}$	$D_{1,3,4}$
$\|\Delta\mathbf{f}\|_\infty$	1.1303	1.1309	1.1320	1.1308	1.1319	1.1319
Region	$D_{1,4,1}$	$D_{1,4,2}$	$D_{1,4,3}$	$D_{1,4,4}$	$D_{2,1,1}$	$D_{2,1,2}$
$\|\Delta\mathbf{f}\|_\infty$	1.1307	1.1305	1.1318	1.1323	1.1330	1.1329
Region	$D_{2,1,3}$	$D_{2,1,4}$	$D_{2,2,1}$	$D_{2,2,2}$	$D_{2,2,3}$	$D_{2,2,4}$
$\|\Delta\mathbf{f}\|_\infty$	1.1298	1.1298	1.1326	1.1328	1.1301	1.1302
Region	$D_{2,3,1}$	$D_{2,3,2}$	$D_{2,3,3}$	$D_{2,3,4}$	$D_{2,4,1}$	$D_{2,4,2}$
$\|\Delta\mathbf{f}\|_\infty$	1.1321	1.1310	1.1318	1.1322	1.1312	1.1304
Region	$D_{2,4,3}$	$D_{2,4,4}$	$D_{3,1,1}$	$D_{3,1,2}$	$D_{3,1,3}$	$D_{3,1,4}$
$\|\Delta\mathbf{f}\|_\infty$	1.1319	1.1324	1.1321	1.1324	1.1308	1.1303
Region	$D_{3,2,1}$	$D_{3,2,2}$	$D_{3,2,3}$	$D_{3,2,4}$	$D_{3,3,1}$	$D_{3,3,2}$
$\|\Delta\mathbf{f}\|_\infty$	1.1319	1.1321	1.1309	1.1307	1.1309	1.1310
Region	$D_{3,3,3}$	$D_{3,3,4}$	$D_{3,4,1}$	$D_{3,4,2}$	$D_{3,4,3}$	$D_{3,4,4}$
$\|\Delta\mathbf{f}\|_\infty$	1.1319	1.1318	1.1303	1.1305	1.1323	1.1324
Region	$D_{4,1,1}$	$D_{4,1,2}$	$D_{4,1,3}$	$D_{4,1,4}$	$D_{4,2,1}$	$D_{4,2,2}$
$\|\Delta\mathbf{f}\|_\infty$	1.1320	1.1317	1.1308	1.1309	1.1317	1.1314
Region	$D_{4,2,3}$	$D_{4,2,4}$	$D_{4,3,1}$	$D_{4,3,2}$	$D_{4,3,3}$	$D_{4,3,4}$
$\|\Delta\mathbf{f}\|_\infty$	1.1311	1.1312	1.1307	1.1308	1.1320	1.1320
Region	$D_{4,4,1}$	$D_{4,4,2}$	$D_{4,4,3}$	$D_{4,4,4}$		
$\|\Delta\mathbf{f}\|_\infty$	1.1303	1.1305	1.1323	1.1322		

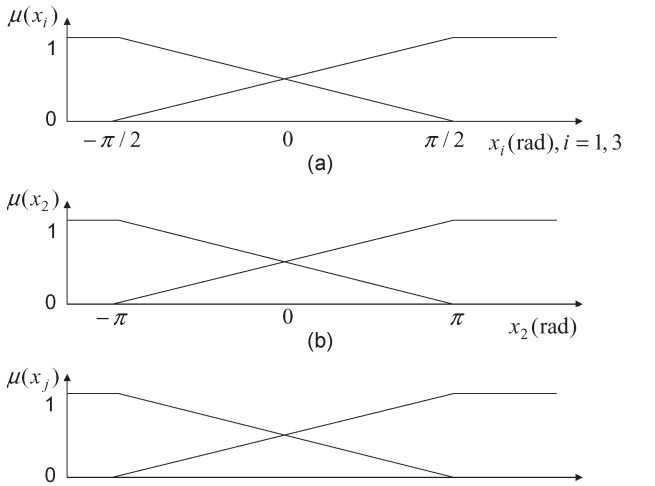

Fig. 2. Membership functions for the system states $x_1, \ldots, x_6$ in Case B.

B. Case for Six Premise Variables

The operating points, in this case, are chosen in the form of $\{\mathbf{x}_{i_1,i_2,i_3,i_4,i_5,i_6} = (x_{1,i_1}, x_{2,i_2}, x_{3,i_3}, x_{4,i_4}, x_{5,i_5}, x_{6,i_6})^{\mathrm{T}} | 1 \le i_j \le n_j$ and n_j are positive integers for $j = 1, \ldots, 6\}$. In this

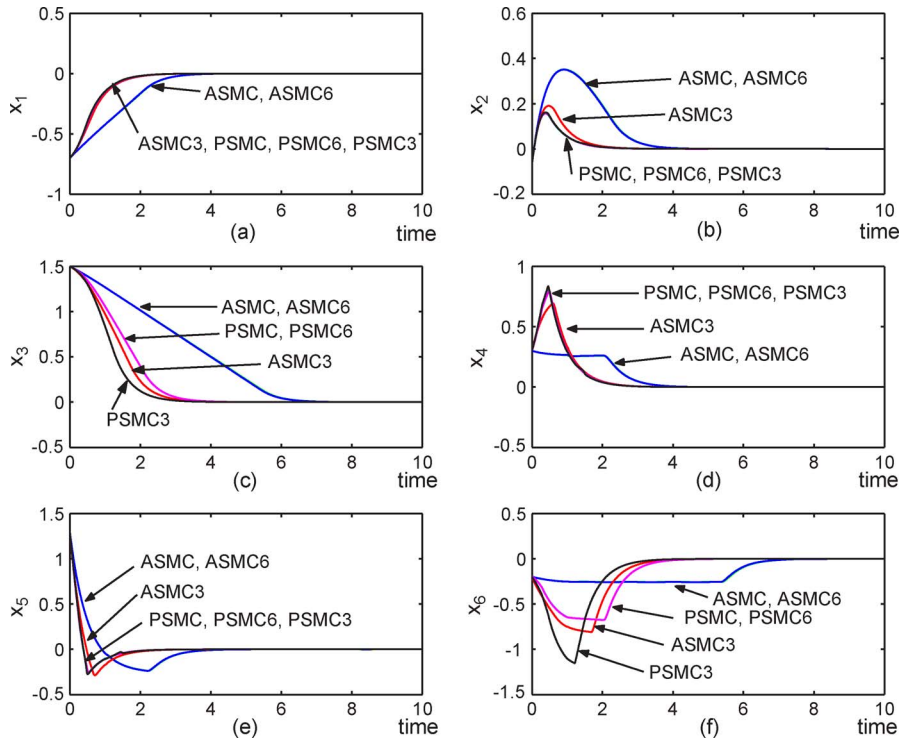

Fig. 3. Time history of the six system states.

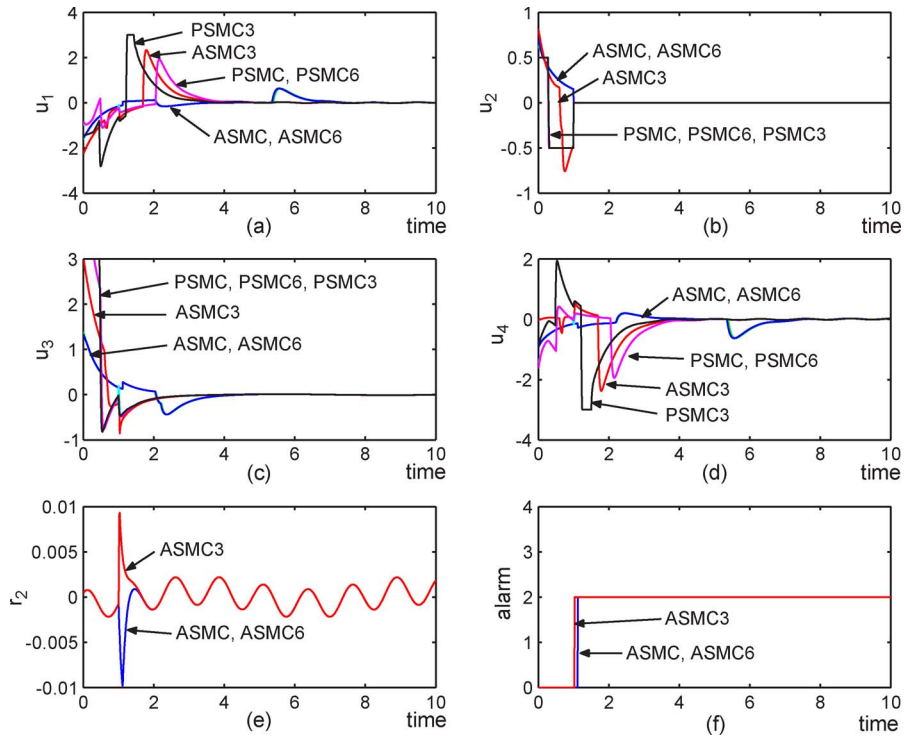

Fig. 4. Time history of (a)–(d) the four control inputs, (e) the residual signals r_2, and (f) the alarm signals.

example, we select $n_j = 2$ for $j = 1, \ldots, 6$ and also employ the triangular membership functions as shown in Fig. 2. Under these settings, we have $2^6 = 64$ operating points and 64 linear local models which are determined from the relation $A_{i_1,i_2,i_3,i_4,i_5,i_6} = F(\mathbf{x}_{i_1,i_2,i_3,i_4,i_5,i_6})$. The associated T–S model can also be easily determined. Details are omitted. Since the T–S-type controller uses six premise variables for this case, it triggers 64 rules (i.e., 2^6 linear models) at each time instant. Furthermore, it does not create an extra online computational burden if the partition for the regions of the system states is made finer, as seen in the previous case. Moreover, it is found that $\|\Delta \mathbf{f}\|_\infty \approx 0.005$, which can be offline computed. This implies that the difference between the T–S model and the original dynamics for this case is much smaller than that

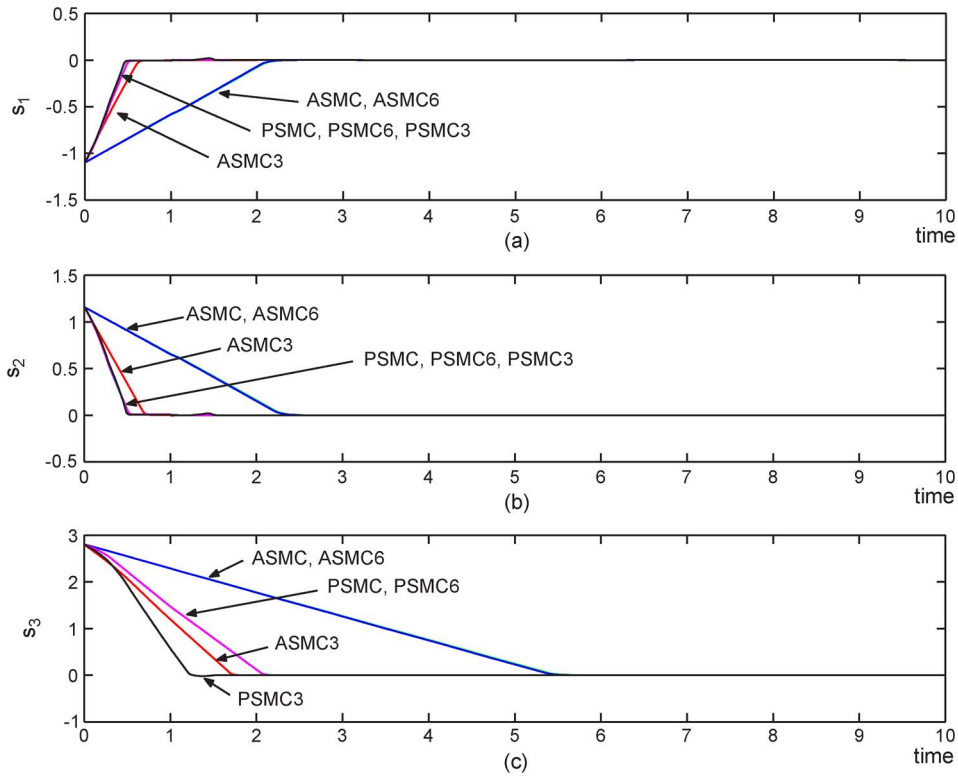

Fig. 5. Time history of the sliding variables.

TABLE II
PERFORMANCES OF THE SIX SMC RELIABLE SCHEMES

	ASMC	PSMC	ASMC3	PSMC3	ASMC6	PSMC6
$\|\|\mathbf{u}\|\|_\infty$	2.3849	3.5291	3.8461	4.2551	2.3536	3.5516
$\int \mathbf{u}^T\mathbf{u}$	1.9306	8.1333	7.9844	15.4786	1.9397	8.1817
$\int \mathbf{x}^T\mathbf{x}$	6.1043	3.9646	3.8049	3.7625	6.0872	3.9635

of Case A, although this case consumes more time (since it triggers 64 rules at every time instant) to evaluate the T–S model than that of Case A (only triggers eight rules at each time instant).

Numerical results are shown in Figs. 3–5 and Tables I and II. Among these, we use the following six control schemes: the first two contain the active and the passive SMC reliable designs adopted from [19] (labeled ASMC and PSMC, respectively), while the others are the active and the passive T–S model-based SMC reliable schemes using 3 and 6 premise variables, respectively, as stated in Cases A and B above (labeled ASMC3, PSMC3, ASMC6 and PSMC6, respectively). The parameters of these SMC reliable designs are set to be $M = 2I_3$, $\eta = 0.5$, $\mathbf{d} = (0.01\sin(t), 0.01\cos(t), 0.01\cos(5t))^{\mathrm{T}}$, $\nu = 0.5$, $\mathbf{x}(0) = (-0.7, -0.07, 1.5, 0.3, 1.3, -0.2)^{\mathrm{T}}$, and the sign function is replaced by the saturation function with a boundary layer width of 0.05 to alleviate the chattering produced by the sign function. Meanwhile, the upper bounds $\rho(\mathbf{x}, t)$ and $\rho_p(\mathbf{x}, t)$ in Remark 2 are selected to be $\|\Delta\mathbf{f}\|_\infty + \|\mathbf{d}\|_\infty$ and $\|\Delta\mathbf{f}\|_\infty + \|G_\mathcal{F}\| + \|\mathbf{d}\|_\infty$, respectively, where $\|\mathbf{d}\|_\infty := \sup_t \|\mathbf{d}\|$. In addition, we adopt the same observer and observer parameters from [19, eqs. (10) and (11), p. 335] as the FDD mechanism for active reliable mission. The observer was shown to be able to reflect the fault of any single actuator at an exponential rate. Before alarm, all of the active reliable schemes adopt their conventional nonreliable designs as if all the actuators are available. For instance, the nonreliable T–S-based SMC controller has the form of (15), (16), and (20) with all the actuators being healthy. When there is an alarm, the associated active reliable controllers are activated according to the FDD information. To demonstrate reliable performance, we assume that u_2 fails at $t = 1$ so that $\mathcal{H} = \{u_1, u_3, u_4\}$ and $\mathcal{F} = \{u_2\}$, and that all of the passive schemes are designed by considering u_2 as the susceptible actuator. The threshold for the alarm is set to be 0.01, i.e., the alarm is fired if the magnitude of any of the residual signals from the observer is greater than 0.01.

It is shown in Fig. 3 that the stabilization performance is, as expected, achieved for all of the six control schemes. However, since the T–S model for Case B is very close to the original nonlinear model ($\|\Delta\mathbf{f}\|_\infty \leq 0.005$), the state curves, the sliding variables and the control curves for the active scheme ASMC6 of Case B and the active SMC reliable design ASMC are very close to each other. The same scenario can also be found for the passive schemes PSMC6 and PSMC, as shown in Figs. 3–5. In Fig. 4(e), the actuator fault is successfully detected and diagnosed by all of the three active designs, since the magnitude of the second residual signal exceeds the threshold near $t_{\mathrm{ASMC3}} \approx 1.04$ and $t_{\mathrm{ASMC,ASMC6}} \approx 1.13$, respectively. This can also be seen from the alarm signals shown in Fig. 4(f) where the alarm value 2 denotes the fault of the second actuator. The alarm t_{ASMC3} is a little earlier than t_{ASMC} and t_{ASMC6}, because the initial magnitude of the fault (at $t = 1$) by the scheme ASMC3 is larger than the other two in the relation of $|\Delta u_2|_{\mathrm{ASMC3}} \approx 0.475 > |\Delta u_2|_{\mathrm{ASMC,ASMC6}} \approx 0.15$, which can be verified from Fig. 4(b) and the fact how $|\Delta u_2|$

influences the residual signals (see [19, eq. (15)]). After the fault is successfully detected and diagnosed, the associated active reliable controllers are activated and the magnitude of the residual signals soon decreases, as shown in Fig. 4(e). Due to the lack of FDD information, the passive reliable designs often overestimate the magnitude of faults. Thus, the passive designs require a larger maximum control magnitude $\|\mathbf{u}\|_\infty := \sup_t \|\mathbf{u}(t)\|$ than the active designs do, as can be seen in Table II. Similarly, since the model error between the T–S model of Case A and the original nonlinear model is much larger than that of Case B, the required $\|\mathbf{u}\|_\infty$ and the consumed energy $\int \mathbf{u}^{\mathrm{T}}\mathbf{u}$ for Case A are also larger than those of Case B and the conventional SMC reliable design in both of the active and the passive missions. This can also be found in Table II and Fig. 5, in which the sliding variables of Case A reach the sliding surface faster than those of the other two types of designs. Indeed, the model error between the T–S model of Case A and the original dynamics cannot be made small enough for this example, because Case A only uses the three Euler's angles as premise variables, and there are some terms of the original dynamics that only involve the three angular velocities. Thus, the reliable schemes of Case A require larger $\|\mathbf{u}\|_\infty$ and more $\int \mathbf{u}^{\mathrm{T}}\mathbf{u}$ than the other two types of schemes to compensate for the model error. Although Case A consumes much more energy than the other two types of designs, it experiences a smaller quadratic performance $\int \mathbf{x}^{\mathrm{T}}\mathbf{x}$ (see Table II). It is worth noting from Fig. 4(b) that u_2 fails after $t = 1$ and changes its sign near $t = 0.28$ for all of the three passive schemes. The sign change of u_2 is verified by the sign change of $G_{\mathcal{F}}^{\mathrm{T}}\mathbf{s}$, which agrees with (29). Furthermore, the control input u_2 for the three passive schemes, as shown in Fig. 4(b), has a magnitude of 0.5 before the fault occurs, which agrees with the passive design (29) with $\nu = 0.5$. Finally, when repeatedly computing the controllers 5×10^4 times, the T–S-type design (including the determination of membership weightings) consumes less CPU time than the classic SMC design in the relation of $(\mathrm{CPU})_{\mathrm{ASMC3,PSMC3}} \approx 5.087 \leq (\mathrm{CPU})_{\mathrm{ASMC6,PSMC6}} \approx 7.453 \leq (\mathrm{CPU})_{\mathrm{ASMC,PSMC}} \approx 10.313$. From this example, it is concluded that the proposed T–S-type approach not only alleviates the online computational burden and promotes the success and reliability of real-time implementations [26], it is also able to efficiently perform the stabilization mission as well as the conventional SMC reliable design. Moreover, the T–S model-based SMC schemes do not create an extra online computational burden when the partition of the premise variables is made finer.

V. Conclusion

A T–S model-based SMC reliable design has been presented for a set of second-order nonlinear control systems. The proposed reliable scheme is shown to be able to continue the control mission safely without prompt maintenance and achieve the stabilization performance even when some of the actuators experience outage. Moreover, the presented scheme retains the benefits of both the T–S and the SMC approaches. It not only alleviates the online computational burden since it uses the T–S model to approximate the original nonlinear one and most of the system parameters of the T–S model can be offline computed, but it also preserves the advantages of the SMC schemes, including rapid response and robustness. Moreover, the increase in the partition number of the region of premise variables in this T–S scheme does not create extra online computational burdens for the scheme. Finally, simulation results have demonstrated the benefits of the proposed scheme.

References

[1] R. H. Abiyev and O. Kaynak, "Fuzzy wavelet neural networks for identification and control of dynamic plants—A novel structure and comparative study," *IEEE Trans. Ind. Electron.*, vol. 55, no. 8, pp. 3133–3140, Aug. 2008.

[2] G. Bartolini, A. Ferrara, E. Usai, and V. I. Utkin, "On multi-input chattering-free second-order sliding mode control," *IEEE Trans. Ind. Electron.*, vol. 45, no. 9, pp. 1711–1717, Sep. 2000.

[3] A. Bartoszewicz, "Discrete-time quasi-sliding-mode control strategies," *IEEE Trans. Ind. Electron.*, vol. 45, no. 4, pp. 633–637, Aug. 1998.

[4] W. Chang, J. B. Park, Y. H. Joo, and G. Chen, "Design of robust fuzzy-model-based controller with sliding mode control for SISO nonlinear systems," *Fuzzy Sets Syst.*, vol. 125, no. 1, pp. 1–22, Jan. 2002.

[5] B.-S. Chen, Y.-T. Chang, and Y.-C. Wang, "Robust H_∞-stabilization design in gene networks under stochastic molecular noises: Fuzzy-interpolation approach," *IEEE Trans. Syst., Man, Cybern. B, Cybern.*, vol. 38, no. 1, pp. 25–42, Feb. 2008.

[6] K.-H. Cheng, C.-F. Hsu, C.-M. Lin, T.-T. Lee, and C. Li, "Fuzzy-neural sliding-mode control for DC–DC converters using asymptotic Gaussian membership functions," *IEEE Trans. Ind. Electron.*, vol. 54, no. 3, pp. 1528–1536, Jun. 2007.

[7] H. H. Choi, "Sliding-mode output feedback control design," *IEEE Trans. Ind. Electron.*, vol. 55, no. 11, pp. 4047–4054, Nov. 2008.

[8] L. dos Santos Coelho and B. M. Herrera, "Fuzzy identification based on a chaotic particle swarm optimization approach applied to a nonlinear yo-yo motion system," *IEEE Trans. Ind. Electron.*, vol. 54, no. 6, pp. 3234–3245, Dec. 2007.

[9] M. L. Corradini and G. Orlando, "Actuator failure identification and compensation through sliding modes," *IEEE Trans. Control Syst. Technol.*, vol. 15, no. 1, pp. 184–190, Jan. 2007.

[10] R. A. Decarlo, S. H. Zak, and G. P. Matthews, "Variable structure control of nonlinear multivariable systems: A tutorial," *Proc. IEEE*, vol. 76, no. 3, pp. 212–232, Mar. 1988.

[11] M. O. Efe, O. Kaynak, and B. M. Wilamowski, "Stable training of computationally intelligent systems by using variable structure systems technique," *IEEE Trans. Ind. Electron.*, vol. 47, no. 2, pp. 487–496, Apr. 2000.

[12] G. H. Golub and C. F. Van Loan, *Matrix Computations,* 3rd ed. Baltimore, MD: The Johns Hopkins Univ. Press, 1996.

[13] J. Huang and C.-F. Lin, "Numerical approach to computing nonlinear control laws," *J. Guid. Control Dyn.*, vol. 18, no. 5, pp. 989–994, 1995.

[14] C.-L. Hwang, "A novel Takagi–Sugeno-based robust adaptive fuzzy sliding-mode controller," *IEEE Trans. Fuzzy Syst.*, vol. 12, no. 5, pp. 676–687, Oct. 2004.

[15] P. Ignaciuk and A. Bartoszewicz, "Linear quadratic optimal discrete-time sliding-mode controller for connection-oriented communication networks," *IEEE Trans. Ind. Electron.*, vol. 55, no. 11, pp. 4013–4021, Nov. 2008.

[16] Z. Li, W. A. Halang, and G. Chen, Eds., *Integration of Fuzzy Logic and Chaos Theory*. New York: Springer-Verlag, 2006.

[17] Y.-W. Liang, D.-C. Liaw, and T.-C. Lee, "Reliable control of nonlinear systems," *IEEE Trans. Autom. Control*, vol. 45, no. 4, pp. 706–710, Apr. 2000.

[18] Y.-W. Liang and S.-D. Xu, "Reliable control of nonlinear systems via variable structure scheme," *IEEE Trans. Autom. Control*, vol. 51, no. 10, pp. 1721–1725, Oct. 2006.

[19] Y.-W. Liang, S.-D. Xu, and C.-L. Tsai, "Study of VSC reliable designs with application to spacecraft attitude stabilization," *IEEE Trans. Control Syst. Technol.*, vol. 15, no. 2, pp. 332–338, Mar. 2007.

[20] Y.-W. Liang, S.-D. Xu, D.-C. Liaw, and C.-C. Chen, "A study of T–S model-based SMC scheme with application to robot control," *IEEE Trans. Ind. Electron.*, vol. 55, no. 11, pp. 3964–3971, Nov. 2008.

[21] F. Liao, J. L. Wang, and G.-H. Yang, "Reliable robust flight tracking control: An LMI approach," *IEEE Trans. Control Syst. Technol.*, vol. 10, no. 1, pp. 76–89, Jan. 2002.

[22] C. Lin, Q.-G. Wang, and T. H. Lee, "Stabilization of uncertain fuzzy time-delay systems via variable structure control approach," *IEEE Trans. Fuzzy Syst.*, vol. 13, no. 6, pp. 787–798, Dec. 2005.
[23] H. Marzi, "Modular neural network architecture for precise condition monitoring," *IEEE Trans. Instrum. Meas.*, vol. 57, no. 4, pp. 805–812, Apr. 2008.
[24] S. Mohagheghi, G. K. Venayagmoorthy, and R. G. Harley, "Fully evolvable optimal neurofuzzy controller using adaptive critic designs," *IEEE Trans. Fuzzy Syst.*, vol. 16, no. 6, pp. 1450–1461, Dec. 2008.
[25] *Optimization Toolbox User's Guide, for Use With MATLAB*, Mathworks Inc., Natick, MA, 2001. [Online]. Available: http://www.mathworks.com
[26] P. Quiñones-Reyes, H. Benitez-Pérez, F. Cárdenas-Flores, and F. Garcia-Nocetti, "An approximation for reconfigurable fuzzy Takagi–Sugeno networked control," *IEEE Potentials*, vol. 27, no. 6, pp. 38–44, Nov./Dec. 2008.
[27] A. Šabanović, M. Elitaş, and K. Ohnishi, "Sliding modes in constrained systems control," *IEEE Trans. Ind. Electron.*, vol. 55, no. 9, pp. 3332–3339, Sep. 2008.
[28] R. F. Stengel, "Intelligent failure-tolerant control," *IEEE Control Syst. Mag.*, vol. 11, no. 4, pp. 14–23, Jun. 1991.
[29] S.-C. Tan, Y. M. Lai, and C. K. Tse, "General design issues of sliding-mode controllers in DC–DC converters," *IEEE Trans. Ind. Electron.*, vol. 55, no. 3, pp. 1160–1174, Mar. 2008.
[30] T. Takagi and M. Sugeno, "Fuzzy identification of systems and its applications to modeling and control," *IEEE Trans. Syst., Man, Cybern.*, vol. SMC-15, no. 1, pp. 116–132, 1985.
[31] K. Tanaka and H. O. Wang, *Fuzzy Control Systems Design and Analysis: A Linear Matrix Inequality Approach*. Hoboken, NJ: Wiley, 2001.
[32] R. J. Veillette, J. V. Medanic, and W. R. Perkins, "Design of reliable control systems," *IEEE Trans. Autom. Control*, vol. 37, no. 3, pp. 290–304, Mar. 1992.
[33] M. Vidyasagar and N. Viswanadham, "Reliable stabilization using a multi-controller configuration," *Automatica*, vol. 21, no. 5, pp. 599–602, Sep. 1985.
[34] G.-H. Yang, J. L. Wang, and Y. C. Soh, "Reliable guaranteed cost control for uncertain nonlinear systems," *IEEE Trans. Autom. Control*, vol. 45, no. 11, pp. 2188–2192, Nov. 2000.
[35] X. Yu, B. Wang, Z. Galias, and G. Chen, "Discretization effect on equivalent control-based multi-input sliding-mode control systems," *IEEE Trans. Autom. Control*, vol. 53, no. 6, pp. 1563–1569, Jul. 2008.
[36] W. Wang, "An intelligent system for machinery condition monitoring," *IEEE Trans. Fuzzy Syst.*, vol. 16, no. 1, pp. 110–122, Feb. 2008.
[37] W. Zhou, T. G. Habetler, and R. G. Harley, "Bearing fault detection via stator current noise cancellation and statistical control," *IEEE Trans. Ind. Electron.*, vol. 55, no. 12, pp. 4260–4269, Dec. 2008.

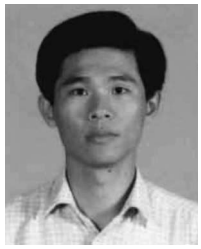

Yew-Wen Liang (M'02) was born in Taiwan in 1960. He received the B.S. degree in mathematics from Tung Hai University, Taichung, Taiwan, in 1982, and the M.S. degree in applied mathematics and the Ph.D. degree in electrical and control engineering from National Chiao Tung University, Hshinchu, Taiwan, in 1984 and 1998, respectively.

Since August 1987, he has been with National Chiao Tung University, where he is currently an Associate Professor of electrical and control engineering. His research interests include nonlinear control systems, reliable control, and fault detection and diagnosis issues.

Sheng-Dong Xu (S'02) received the Ph.D. degree in electrical engineering and control engineering from National Chiao Tung University, Hsinchu, Taiwan, in 2009.

He is currently a faculty member of the Department of Computer Science, National Chengchi University, Taipei, Taiwan. His research interests include control engineering, embedded systems, and industrial electronics.

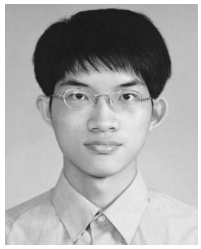

Li-Wei Ting received the M.S. degree in electrical engineering and control engineering from National Chiao Tung University, Hsinchu, Taiwan, in 2009.

He is currently with National Chiao Tung University. His research interests include control engineering, fuzzy systems, and industrial electronics.